Water Resources Research

RESEARCH ARTICLE
10.1029/2024WR038341

Anthropogenic and Hydroclimatic Controls on the CO_2 and CH_4 Dynamics in Subtropical Monsoon Rivers

Shuai Chen[1], Lishan Ran[1], Clément Duvert[2], Boyi Liu[1], Yongli Zhou[1], Xiankun Yang[3], Qianqian Yang[1], Yuxin Li[1], and Si-Liang Li[4]

[1]Department of Geography, The University of Hong Kong, Hong Kong, China, [2]Research Institute for the Environment and Livelihoods, Charles Darwin University, Darwin, NT, Australia, [3]School of Geography and Remote Sensing, Guangzhou University, Guangzhou, China, [4]Institute of Surface-Earth System Science, School of Earth System Science, Tianjin University, Tianjin, China

Key Points:

- Land use and aquatic metabolism greatly regulate the riverine CO_2 and CH_4 dynamics
- Seasonal pCO_2 and pCH_4 variations are strongly governed by hydroclimatic conditions
- Urbanization and climate warming will further enhance riverine CH_4 and CO_2 emissions

Supporting Information:

Supporting Information may be found in the online version of this article.

Correspondence to:

L. Ran,
lsran@hku.hk

Citation:

Chen, S., Ran, L., Duvert, C., Liu, B., Zhou, Y., Yang, X., et al. (2025). Anthropogenic and hydroclimatic controls on the CO_2 and CH_4 dynamics in subtropical monsoon rivers. *Water Resources Research*, *61*, e2024WR038341. https://doi.org/10.1029/2024WR038341

Received 3 JUL 2024
Accepted 11 DEC 2024
Corrected 21 JAN 2025

This article was corrected on 21 JAN 2025. See the end of the full text for details.

Author Contributions:

Conceptualization: Shuai Chen, Lishan Ran
Funding acquisition: Lishan Ran
Investigation: Shuai Chen, Boyi Liu, Xiankun Yang
Methodology: Boyi Liu, Qianqian Yang, Yuxin Li
Supervision: Lishan Ran
Visualization: Yongli Zhou
Writing – original draft: Shuai Chen
Writing – review & editing: Lishan Ran, Clément Duvert, Si-Liang Li

Abstract Anthropogenic perturbations have substantially altered riverine carbon cycling worldwide, exerting influences on dissolved carbon dioxide (CO_2) and methane (CH_4) dynamics at multiple levels. However, the magnitude and role of anthropogenic activities in modulating carbon emissions across entire river networks, as well as the influence of climatic controls, remain largely unresolved. Here, we explore the controlling factors of riverine CO_2 and CH_4 dynamics across 62 subtropical, monsoon-influenced streams and rivers through basin-wide seasonal measurements. We found that land use and aquatic metabolism played significant roles in regulating the spatial and temporal patterns of both gases. Increased nutrient levels and organic matter contributed to higher partial pressure of CO_2 (pCO_2) and CH_4 (pCH_4). Dissolved oxygen, stable carbon isotope of dissolved inorganic carbon, the proportion of impervious surface, catchment slope, and river width were the major predictors for pCO_2. For pCH_4, the major predictors were Chlorophyll *a* and water temperature, which influence organic matter availability and methanogenesis. Seasonal variations in pCO_2 and pCH_4 were strongly modulated by hydroclimatic conditions, with temperature markedly regulating river ecosystem metabolism. These findings highlight the likelihood of significant changes in riverine carbon emissions as climate changes and land use patterns evolve, thereby profoundly affecting the global carbon cycle.

1. Introduction

Rivers and streams serve as vital active conduits in connecting terrestrial, atmospheric, and marine carbon reservoirs, and they play a crucial role in carbon emissions from freshwater ecosystems (Battin et al., 2023; Raymond et al., 2013; Rosentreter et al., 2021). A recent study has updated the CO_2 emissions from global rivers and streams to be 2.0 Pg C per year by considering seasonal variations in catchment biogeochemistry and hydrology (Liu et al., 2022). Another recent estimate by Lauerwald et al. (2023) reveals that rivers and streams are the largest contributor (~84%) to the CO_2 emissions from global inland waters. Furthermore, a more recent work on CH_4 emissions from streams and rivers based on global data compilations shows that global rivers and streams are emitting CH_4 at a rate of approximately 20.9 Tg C yr^{-1} (Rocher-Ros et al., 2023), which represents nearly half of the total emissions from lake and reservoir systems (Johnson et al., 2021, 2022). These findings underscore the disproportionately significant role of running waters in carbon emissions, considering their relatively small areal extent (Allen & Pavelsky, 2018). These continuous efforts to refine carbon budget estimates highlight the importance of unraveling the biogeochemical processes that govern riverine carbon dynamics in a rapidly changing world.

The biogeochemical processes governing CO_2 and CH_4 dynamics in river systems are influenced by a multitude of environmental factors that encompass the production, consumption, exchange, and transport of gases. These factors include oxygen conditions, organic matter availability, geomorphological characteristics, land use/land cover, soil characteristics, hydrological connections, and climate variables such as temperature and runoff (Battin et al., 2023; Rocher-Ros et al., 2023). Particularly, the widespread impact of human activities on riverine carbon dynamics has received increasing attention worldwide in recent years (Regnier et al., 2022; Xu et al., 2024). Urban and agricultural river systems typically exhibit 'anthropogenically enhanced' carbon cycling due to substantial inputs of nutrients and organic carbon (OC) resulting from surface erosion, leaching, wastewater discharge, and chemical fertilizer use (Park et al., 2018). In most cases, these additional inputs to river systems will promote the production of CO_2 and CH_4. Agricultural activities generate significant amounts of fine

sediments, which contribute to carbon-rich and anoxic stream beds, thereby favoring CH_4 production (Stanley et al., 2016; Zhu et al., 2022). Furthermore, the construction of large-scale reservoirs for hydropower, flood control, and irrigation has substantially modified the greenhouse gas (GHG) dynamics in running waters (Regnier et al., 2022). For instance, dam regulation can lead to high OC burial rates and alter the water level and surface area in upstream and drawdown regions (Maavara et al., 2020), thereby influencing carbon emissions in the impacted areas. Nevertheless, the biogeochemical processes associated with these changes remain poorly understood and necessitate further investigations. Most recent studies assessing the effects of human activities on aquatic carbon cycling have been limited to small- and medium-sized catchments (Herrero Ortega et al., 2019; Zhang et al., 2021; Zhu et al., 2022), and larger-scale, whole-basin studies are now required. Improving our understanding of the anthropogenic impacts on carbon emissions in large basins will be key to predict future changes in global carbon emissions and propose effective mitigation strategies.

Global climate change is known to affect riverine carbon emissions worldwide (Regnier et al., 2022). With further warming, it is projected that global river systems will experience simultaneous and multifaceted changes in hydrology (e.g., runoff and discharge) and temperature (Lee et al., 2023). Elevated temperatures have been widely observed to stimulate the production of CO_2 through increased organic matter respiration rates (Hursh et al., 2017) and the production of CH_4 through enhanced microbial methanogenesis activities (Yvon-Durocher et al., 2014). Increased runoff and discharge have been associated with higher OC export from terrestrial ecosystems to river networks (Laudon et al., 2012), which in turn serves as a crucial substrate for the production of CO_2 and CH_4 through microbial mineralization (Marx et al., 2017; Stanley et al., 2016). Previous research has predominantly focused on the climatic impacts on CO_2 and CH_4 dynamics in boreal (Campeau & Del Giorgio, 2014; Hutchins et al., 2019) and alpine rivers (Zhang, Xia, et al., 2020), where climate changes are expected to be more pronounced. In contrast, less attention has been given to subtropical and tropical rivers, although they act as hotspots for GHG emissions (Borges, Darchambeau, et al., 2015; Liu et al., 2022). Particularly, recent research suggests that the impacts of future climate changes in these regions may have been underestimated (Eccles et al., 2019; Freychet et al., 2021). Given the crucial role played by subtropical and tropical rivers in the global carbon cycle, even minor fluctuations in climate and hydrology can result in substantial changes in carbon emissions. However, there is a dearth of knowledge regarding the effects of climate change on carbon emission dynamics in subtropical and tropical river systems.

In this study, we examined the spatiotemporal dynamics of surface water CO_2 and CH_4 concentrations in 62 catchments across the subtropical Pearl River Basin (PRB) in south China. These catchments span eight Strahler orders. The objectives of this study were (a) to investigate the spatial-temporal patterns of the dissolved CO_2 and CH_4 concentrations in the PRB, (b) to identify the dominant controlling factors for both gases, including geomorphology, climate and hydrology, land uses, soil characteristics, and water chemistry, and (c) to assess the impacts of anthropogenic and climatic factors on the riverine CO_2 and CH_4 dynamics in the PRB. Based on constructed empirical models, we further projected future changes in riverine CH_4 concentrations within the PRB under rising temperatures in a warming world.

2. Materials and Methods

2.1. Study Area and Sampling Overview

The Pearl River is the second largest river in China in terms of discharge, draining roughly 450,000 km^2 and discharging approximately 356 km^3 of water annually to the South China Sea (China River Sediment Bulletin, http://xxzx.mwr.gov.cn/xxgk/gbjb/, last access: 18 December 2023; Figure 1). It is a composite river system formed by the Xijiang, Beijiang, and Dongjiang rivers. The Pearl River Basin (PRB) features a subtropical monsoon climate characterized by hot and humid summers and warm and dry winters, with long-term mean annual precipitation of 1,429 mm yr^{-1} (Tian & Yang, 2017) and approximately 80% of the annual precipitation occurring during the wet season (April to September). Elevations within the PRB range from ~0 to 2,800 m. The western part of the PRB encompasses the Yungui Plateau, while the central region is characterized by a diverse landscape of hills and basins. Extensive carbonate rocks underlie the PRB, particularly in the upper reaches of the Xijiang River, which is renowned as the world's largest karst area. In terms of land cover, the PRB is predominantly occupied by forests, followed by croplands, grasslands, and urban areas. The PRB has also witnessed extensive construction of reservoirs and dams, especially in the Xijiang River Basin.

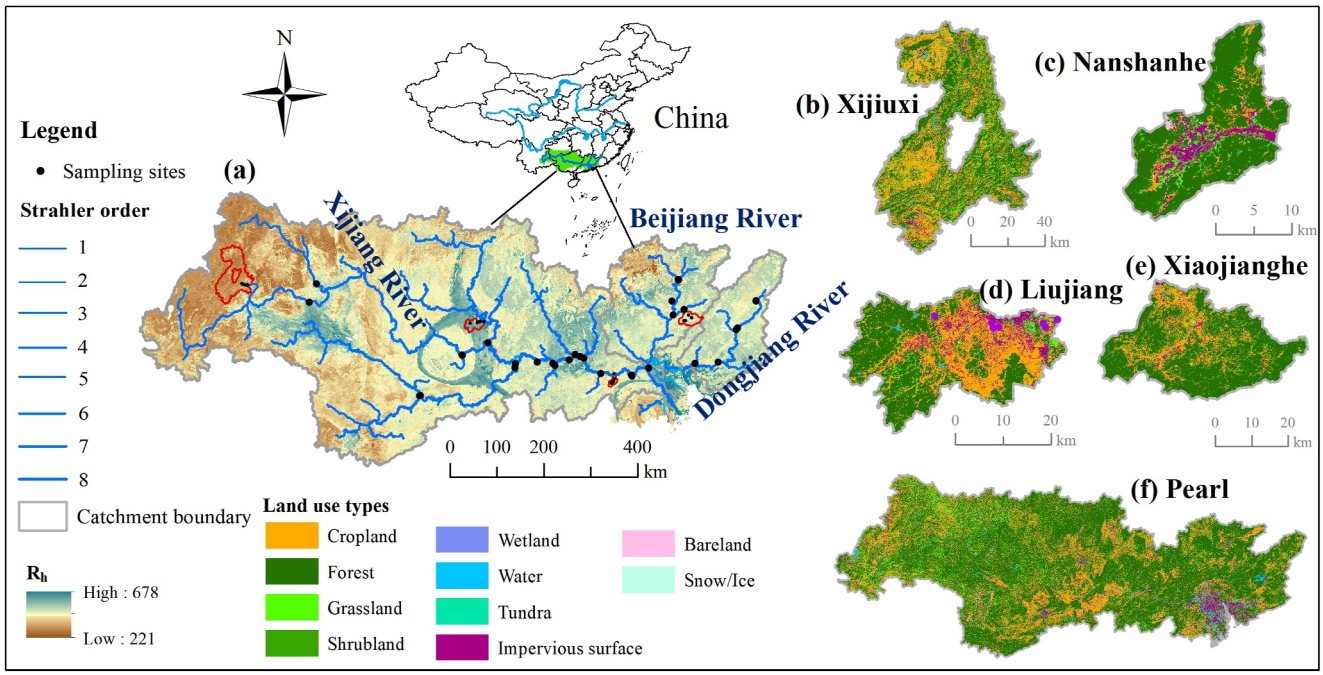

Figure 1. Location map depicting the distribution of (a) heterotrophic soil respiration (R_h) and (b, c, d, e, and f) land use types of the sampling catchments ($n = 62$) within the Pearl River Basin (PRB). The Pearl River system is primarily composed of three major tributaries: the Xijiang, Beijiang, and Dongjiang rivers, with a total of 31 sampling sites situated along the three tributary channels. Furthermore, an additional 31 sites are located in four small catchments (catchment boundary was shown in red in panel) (a), including the (b) Xijiuxi (XJX), (c) Nanshanhe (NSH), (d) Liujiang (LJ), and (e) Xiaojianghe (XJH) rivers.

To investigate the potential drivers of surface water pCO_2 and pCH_4 in the 62 study catchments, their catchment attributes were extracted using ESRI ArcGIS 10.8 (Table S1 in Supporting Information S1). These catchments are widely distributed across the PRB and exhibit significant spatial heterogeneity in topography, lithology, hydrology, and land cover. Among these catchments, four are located in small catchments (i.e., Nanshanhe (NSH), Liujiang (LJ), Xijiuxi (XJX), and Xiaojianghe (NSH); Figure 1) and the remaining cover the mainstem channel of the Xijiang, Beijiang, and Dongjiang rivers. Although agricultural land accounts for a relatively high proportion (20–42%) within the XJX catchment, our sampling sites in this catchment are all located near the outlet which is predominantly forested. Therefore, compared to the other three headwater catchments, we refer to the XJX as a forested catchment. This classification is further supported by our data analysis (e.g., dissolved organic carbon (DOC), pCO_2, and pCH_4) as discussed below.

2.2. Field Sampling and Laboratory Analysis

A total of 124 samples were collected in both large rivers ($n = 31$; Strahler orders 5–8; including the mainstem channel and major tributaries of the Xijiang River, Beijiang River, and Dongjiang River) and small streams ($n = 31$; Strahler orders 1–5; including two urban river systems, a forested river system, and an agricultural river system) within the PRB during daylight hours in summer (July 19th to August 3rd; wet season) and winter (December 7th to 22nd; dry season) of 2021 (Figure 1). To minimize the impact of diurnal variations of pCO_2 and pCH_4 at each sampling site, we attempted to conduct the field sampling at the same time of a day during the two sampling campaigns. Surface water pCO_2 and pCH_4 were determined by the headspace equilibrium method (Campeau et al., 2014). A 100 ml syringe was used to draw 50 ml of stream water, leaving the remaining 50 ml as headspace filled with ambient air. The syringe was then tightly sealed and equilibrated by shaking vigorously for 3 min. Subsequently, 20 ml of the headspace air was transferred into a pre-evacuated 12 ml vial for laboratory analysis. CO_2 and CH_4 concentrations (in duplicate with a repeatability higher than 95%) were analyzed using a gas chromatograph (GC-2010, Shimadzu, Japan) equipped with a flame ionization detector and a methanizer. Calibration of gas concentrations was done using three commercial gas standards (500, 1,000, and 3,000 ppm for

CO_2 and 2, 8, and 100 ppm for CH_4). The correction method proposed by Koschorreck et al. (2021) was employed to calculate the surface water pCO_2, which is crucial for obtaining unbiased measurements. The surface water pCH_4 was calculated based on the headspace ratio and the measured ambient air pCH_4 (details were provided in Supporting Text S1 in Supporting Information S1). Additionally, an investigation was conducted on various surface water quality variables, including dissolved oxygen (DO), water temperature (T_w), pH, dissolved inorganic carbon (DIC) and its stable carbon isotope ($\delta^{13}C_{DIC}$), Chlorophyll a (Chl *a*), total phosphorus (TP), total nitrogen (TN), DOC, and particulate organic carbon (POC) (see Supporting Text S2 in Supporting Information S1 for details).

2.3. Statistical Analyses

We built multiple linear regression models to assess the combined effects of environmental factors on pCO_2 and pCH_4. To obtain optimal predictions of pCO_2 and pCH_4 and assess the relative significance of environmental factors, a comprehensive model incorporating all potential explanatory variables (see Text S3 in Supporting Information S1 for details) was constructed. Data exploration was performed following the protocol described in Zuur et al. (2010) (Text S3 in Supporting Information S1). All predictors included in the initial model were categorized into six groups: (a) general water chemistry (e.g., pH, DO, TN, and TP), (b) carbon species (e.g., $\delta^{13}C_{DIC}$, DOC, POC, Chl *a*, and DIC; Chl *a* was included in this group to better meet the requirement of the path model as discussed below), (c) hydrology and climate (e.g., T_w and runoff), (d) land use (e.g., forest, grassland, shrubland, wetland, and impervious surface), (e) soil characteristics (e.g., crop soil erosion and R_h), and (f) geomorphology (e.g., river width, catchment slope, and channel slope).

Model selection was performed based on corrected Akaike's information criterion (AICc; $\Delta AICc < 2$) to identify the best predictors of pCO_2 and pCH_4 using the *R* package *MuMIn* (Barton & Barton, 2015). Furthermore, model averaging was conducted according to AICc weights when multiple models were selected for parameter estimation and determination of the associated *p*-values by utilizing the function model.avg. All predictors and response variables were standardized using the Z-score before analysis to interpret parameter estimates on a comparable scale. Variance decomposition analysis was conducted based on Z-scores to determine the relative effects of each environmental factor. We then utilized the parameter estimates of interacting predictors to demonstrate the influence of climate (especially water temperature) and in-stream metabolism (represented by DO) on pCH_4. We further examined the combined effects of T_w and DO on pCH_4 by keeping the parameter estimates of all other predictors fixed at their mean value (i.e., 0 as all predictors were Z-scored). The final models were employed for predicting surface water pCO_2 and pCH_4.

We also developed a partial least squares path model (PLS-PM) using the *R* package *plspm* (Sanchez, 2013) to assess the direct and indirect effects of multiple environmental factors on surface water pCO_2 and pCH_4. PLS-PM is a powerful tool for conducting multivariate analyses to investigate intricate cause-effect relationships among multiple latent variables (Du et al., 2023). Each latent variable (e.g., general water chemistry) comprises one or more manifest variables (e.g., DO and pH). In this study, the environmental factors incorporated into the model were divided into seven latent variables, encompassing geomorphology, hydrology and climate, land uses, soil characteristics, carbon species, general water chemistry, and pCO_2 or pCH_4. The selection of the environmental factors and their corresponding manifest variables included in the path model was mainly based on the crucial variables identified through multiple linear regression analysis. PLS-PM was conducted based on the reduction of the full models (initial models with a larger number of variables) to ensure compliance with the PLS-PM analysis requirements. A nonparametric bootstrapping with 1,000 resamples was employed to determine the significance of the path coefficients. All analyses were conducted using *R* software (version 4.3.2, R Development Core Team, 2020).

Data normality was examined using the Shapiro-Wilk normality test. Different groups of data were compared using the Mann-Whitney U and Kruskal-Wallis tests followed by Bonferroni correction for adjusted *p*-values. Simple linear regressions were conducted using Origin (Pro) 2024 to evaluate the correlations between the measured pCO_2 (pCH_4) and the modeled pCO_2 (pCH_4), as well as to investigate the relationships among environmental variables and their correlations with pCH_4/pCO_2. All statistical analyses were performed at a significance level of 0.05. Considering the significant impact of outliers on aquatic CO_2 and CH_4 concentrations, median ± standard deviation (SD) values were preferred over means ±SD to represent the data range.

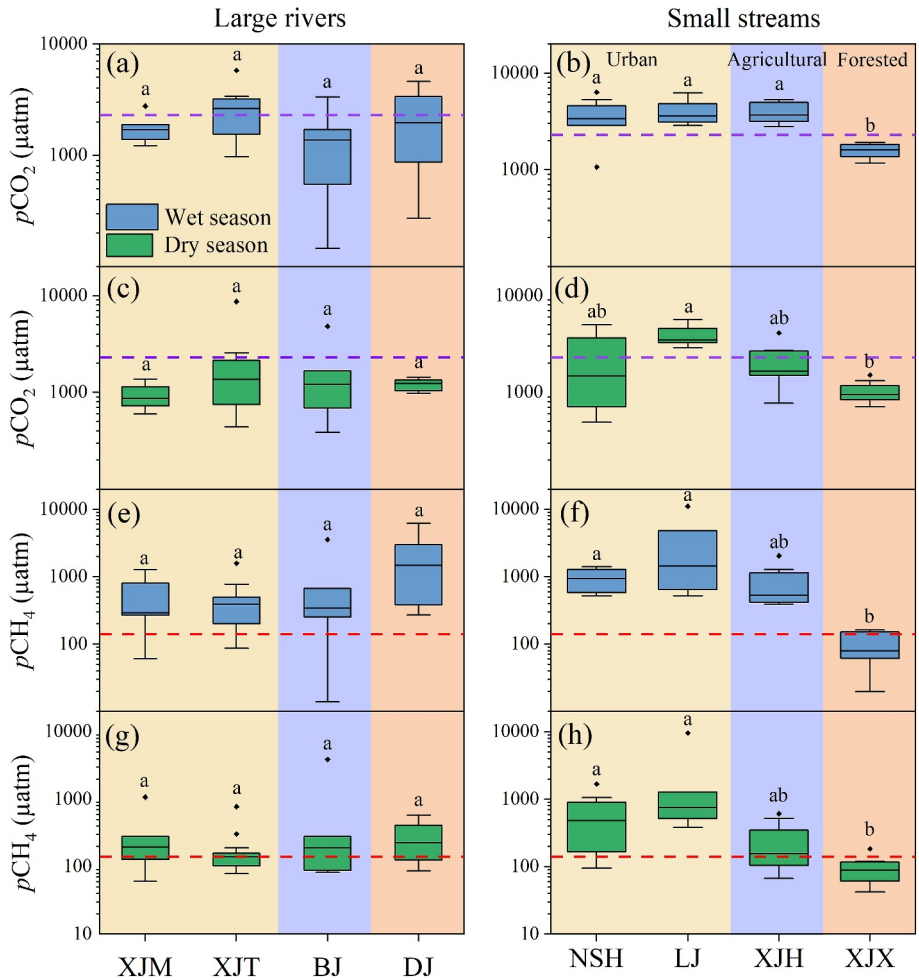

Figure 2. Seasonal variations in (a, b, c, d) pCO_2 and (e, f, g, h) pCH_4 in the three large river basins (XJM and XJT denote the mainstream and major tributaries of the Xijiang River, respectively; BJ=Beijiang; DJ = Dongjiang) and four small catchments (NSH, LJ, XJH, and XJX). The violet and red dotted horizontal lines represent global median pCO_2 (~2,304 µatm) and pCH_4 (~141 µatm) values in rivers (Stanley et al., 2023), respectively. The box represents the 25th and 75th percentiles, the horizontal line in the box represents the median, and the whiskers represent 1.5 times the upper and lower IQR. The solid dots denote the outliers. The letters above the boxes indicate significant differences at the significance level of 0.05.

3. Results

3.1. Spatial and Temporal Variations in Water Quality and Riverine CO_2 and CH_4 Dynamics

Water temperature showed a significant increase during the summer months (wet season; median: 30.1 ± 3.9°C), compared to the winter months (dry season; median: 18.2 ± 1.8°C) (Figure S1a in Supporting Information S1). River water was significantly less oxygenated in the wet season (median: 7.0 ± 1.5 mg L^{-1}) than in the dry season (median: 9.1 ± 1.8 mg L^{-1}) (Figure S1b in Supporting Information S1). Chl *a* exhibited significant variation between the two seasons, with a notably higher median value during the dry season (16.7 ± 20.2 µg L^{-1}) compared to the wet season (median: 8.9 ± 10.2 µg L^{-1}) (Figure S1c in Supporting Information S1). Both riverine pCO_2 and pCH_4 were highly variable, with the pCO_2 varying from 146 to 8,708 µatm and the pCH_4 from 14 to 11,119 µatm (Figure 2). The pCO_2 and pCH_4 levels did not exhibit significant differences among the Xijiang (including both mainstream (XJM) and major tributaries (XJT)), Beijiang (BJ), and Dongjiang (DJ) rivers during both seasons (Figures 2a–2c and, 2e, and 2g). However, cross-site differences were significant when looking at small streams, with urban and agricultural streams showing relatively higher levels of pCO_2 and pCH_4 compared to forested streams (Figures 2b–2d and, 2f, and 2h). The median pCO_2 in the dry season (1,351 ± 1,488 µatm)

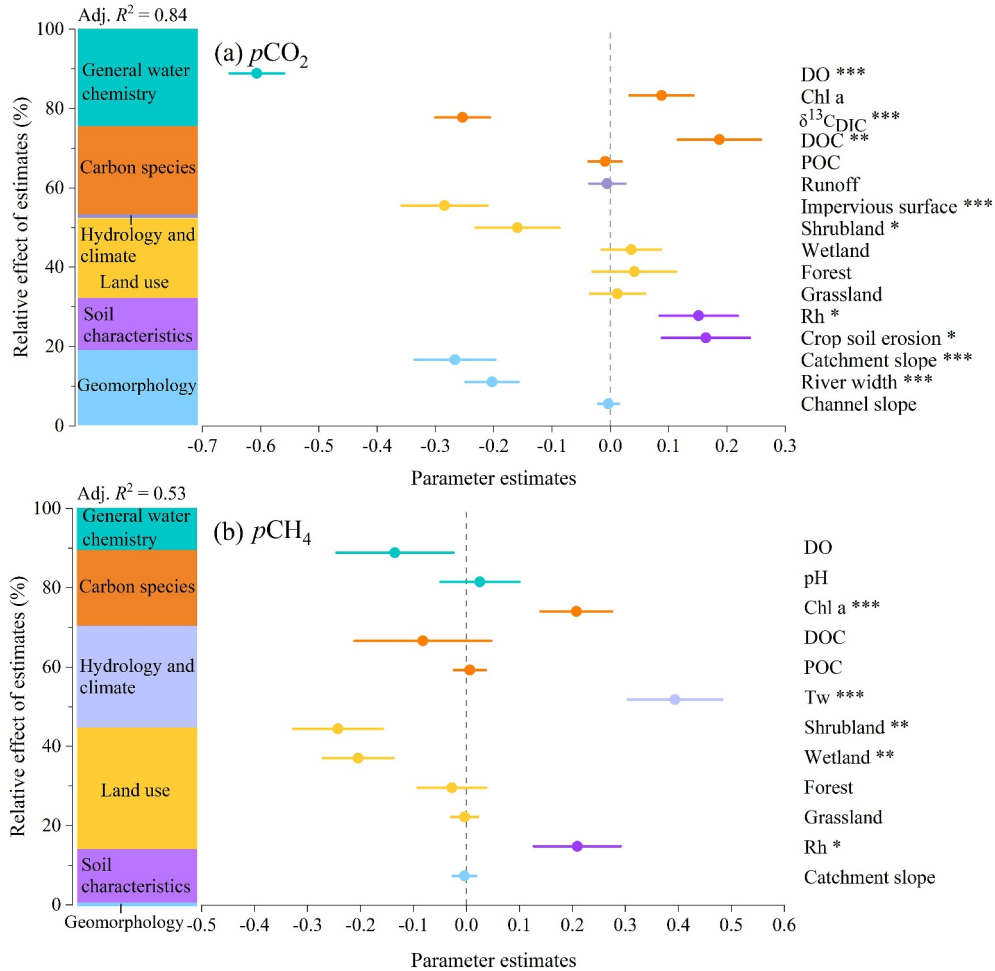

Figure 3. The relative effects of multiple predictors on surface water (a) pCO_2 and (b) pCH_4. The model predictors are represented by averaged parameter estimates (standardized regression coefficients) along with their 95% confidence intervals. The relative importance of each predictor is expressed as a percentage of the variance. The relative effects (in %) of predictors are calculated by taking the ratio between the parameter estimate of a predictor and the sum of all parameter estimates. T_w and R_h represent water temperature and heterotrophic soil respiration, respectively. *$p = < 0.05$, **$p = < 0.01$, ***$p = < 0.001$.

was significantly lower (Mann-Whitney U test; $p < 0.0001$) compared to the wet season (2,789 ± 1,553 μatm). Likewise, the median pCH_4 during the dry season (168 ± 1,721 μatm) was significantly lower (Mann-Whitney U test; $p < 0.0001$) than that in the wet season (495 ± 1,301 μatm).

3.2. Predictors of pCO_2 and pCH_4 and Their Relative Importance

General water chemistry, carbon species, hydrology and climate, land use, soil characteristics, and geomorphology were consistently included in both pCO_2 and pCH_4 models (Figure 3). Collectively, these factors accounted for 84% and 53% of the variance in pCO_2 and pCH_4, respectively. This remarkable explanatory power renders the prediction of surface water pCO_2 and pCH_4 in the PRB feasible and reliable (Figure 4). Among these environmental drivers, general water chemistry was the most influential predictor for pCO_2, accounting for 24.6% of the variance. Carbon species (21.7%), land use (21.6%), geomorphology (19.2%), and soil characteristics (12.8%) also made substantial contributions to the variance in pCO_2 (Figure 3). In comparison, land use (31.0%) and hydrology and climate (25.5%) were the primary drivers for pCH_4. Carbon species (19.2%) played a less important role in influencing pCH_4, followed by soil characteristics (13.6%) and general water chemistry (10.4%) (Figure 3). Additionally, we found significantly negative correlations between surface water pCO_2 and $\delta^{13}C_{DIC}$, as well as DO, along with a significantly positive correlation between pCO_2 and pCH_4 (Figure S2 in Supporting

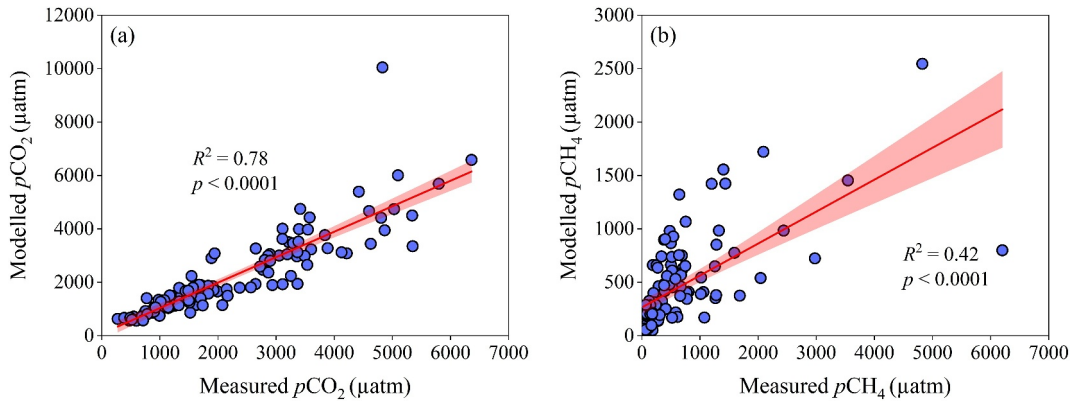

Figure 4. The relationship between measured and modeled values from the selected multiple linear regression models for surface water (a) pCO_2 and (b) pCH_4. Outliers, which are outside of the 1.5 interquartile range, are excluded from analysis. The red shaded area in each panel represents the 95% confidence interval.

Information S1). Furthermore, we observed significant interactions between pCH_4 and both T_w and DO, although the interaction between T_w and pCH_4 was more pronounced (Figures 3b and 6). The effect of T_w on pCH_4 shifted from slightly positive at low temperatures to markedly positive under high temperature conditions. Moreover, the increase in pCH_4 with decreasing DO tends to intensify at lower DO levels (Figure 5).

3.3. Direct and Indirect Effects of Key Factors on pCO_2 and pCH_4

Fourteen manifest variables (i.e., indicators) of environmental factors were retained in the PLS-PM analysis based on the results of the multiple linear regression model (Figure 6). The PLS-PM analysis showed that our model could explain 78% and 46% of the variance in pCO_2 and pCH_4, respectively. Among the examined factors, general water chemistry displayed the most substantial effect on pCO_2, as evidenced by its high path coefficient (−0.92) via direct effects (Figure 6a). Land use also had a significant direct influence on pCO_2 (path coefficient = 0.18). Furthermore, carbon species exerted a significant impact on pCO_2, primarily through indirect regulation on general water chemistry (Figure S3a in Supporting Information S1), and a noteworthy direct effect (path coefficient = 0.19) on pCH_4 (Figure 6b). In contrast, hydrology and climate emerged as the most influential factors (path coefficient = 0.34) in controlling pCH_4 through direct regulation, consistent with our multiple linear regression modeling results. Geomorphology also exhibited, albeit indirectly, a notable effect on pCH_4 (Figure S3b in Supporting Information S1). Additionally, land use displayed a significant direct effect (path coefficient = 0.18) on riverine pCH_4.

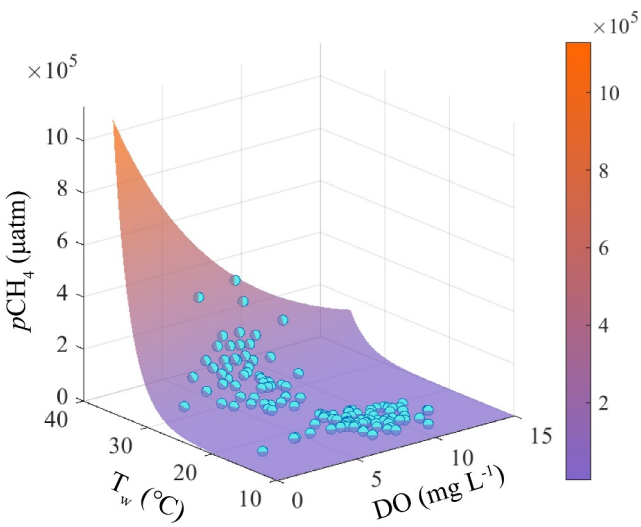

Figure 5. Distribution of the predicted pCH_4 based on the interactive effects of water temperature (T_w) and DO on pCH_4. The color gradient represents the pCH_4 values that range from low (purple) to high (orange). Cyan dots indicate the predicted pCH_4 values corresponding to the measured T_w and DO. Slopes are derived from the outputs of the multiple linear regression model for pCH_4.

4. Discussion

4.1. Complex Environmental Effects on and Common Drivers of pCO_2 and pCH_4

The factors governing the dynamics of riverine CO_2 and CH_4 are complex, as they are closely associated with biogeochemical processes involving the production, delivery, and emission of CO_2 and CH_4 (Gutierrez-Canovas et al., 2024; Mwanake et al., 2022). The results of multiple linear regression models revealed that both pCO_2 and pCH_4 were strongly affected by general water chemistry, carbon species, land use, and soil characteristics (Figure 3). Previous research has demonstrated that water chemistry factors, such as DO and pH, regulate aquatic metabolism (Battin et al., 2023), while carbon species (e.g., OC and Chl *a*), land use, and soil characteristics also play crucial roles (Horgby et al., 2019; Mwanake et al., 2022). The intricate biogeochemical processes governing riverine pCO_2 and pCH_4 were further elucidated by the PLS-PM analysis (Figure 6).

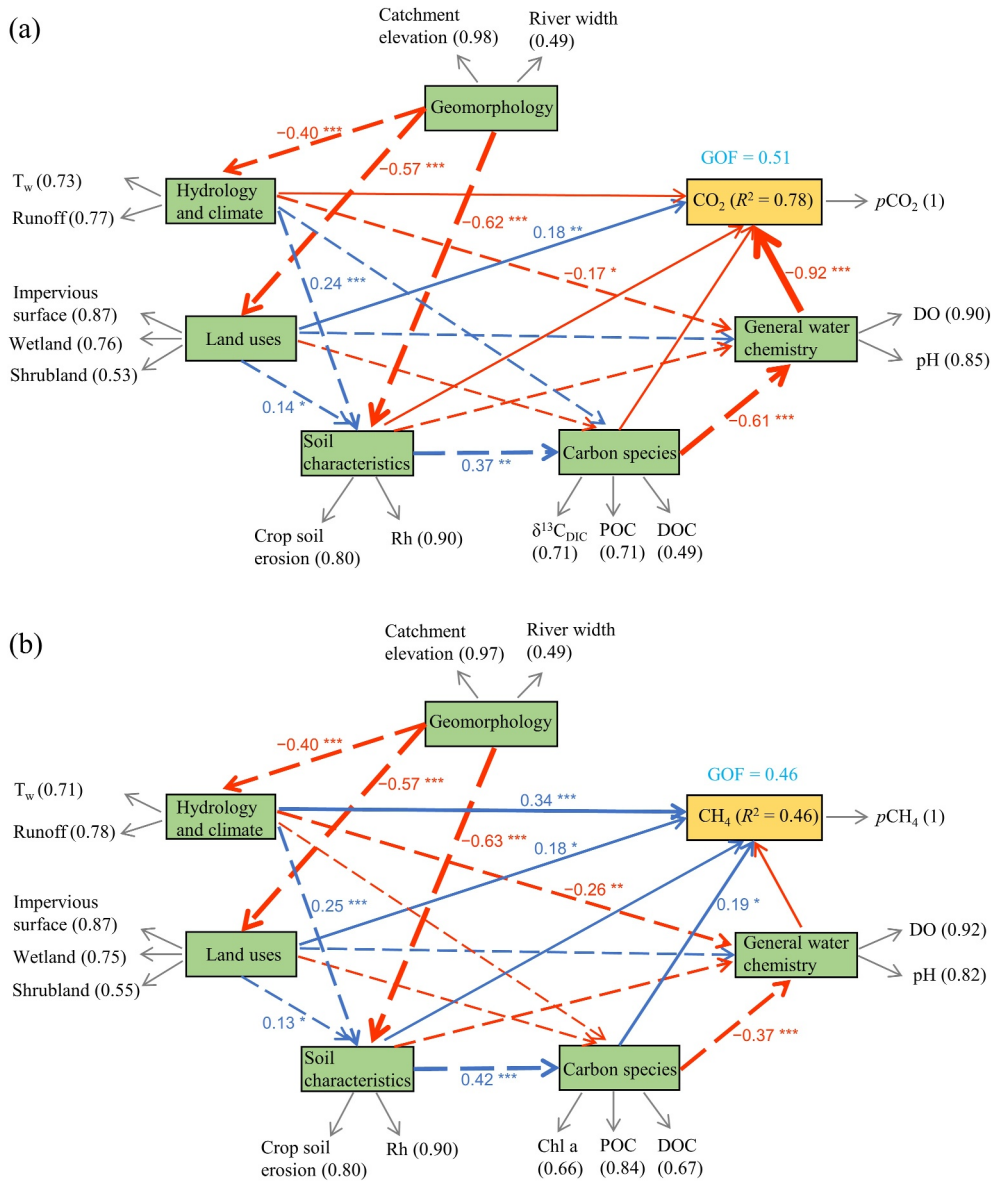

Figure 6. PLS-PM modeling results revealing the direct and indirect effects of key factors on (a) pCO_2 and (b) pCH_4. Path coefficients are represented by arrows, with blue and red arrows indicating positive and negative effects, respectively. Direct and indirect impacts of environmental factors on pCO_2 and pCH_4 are represented by solid and dotted lines, respectively. The latent variable (e.g., land uses) is connected to its indicators (e.g., wetland and shrubland) through gray arrows, with the corresponding loading scores displayed after the indicators. The goodness of fit (GOF) metric assesses the overall fit of the entire model, while the R^2 value quantifies the proportion of variance in pCO_2 and pCH_4 explained by the independent latent variables. The strength of the causal relationship is indicated by the thickness of the line, and significantly different standardized path coefficients are denoted as follows: $*p = < 0.05$, $**p = < 0.01$, $***p = < 0.001$.

Geomorphology is linked to carbon emissions in both direct and indirect ways. First, it directly influences the gas transfer velocity (k) with catchments characterized by higher elevations and steeper slopes generally exhibiting greater k values (Duvert et al., 2018). High k values are typical of headwater streams and often lead to higher CO_2 emissions from these streams relative to larger and lowland rivers (Butman & Raymond, 2011). This aligns with our previous findings that headwater streams (Strahler orders < 3) accounted for 75% of the total CO_2 fluxes in the Pearl River (Chen et al., 2024). Second, geomorphology indirectly affects the availability of OC by influencing land use patterns and hydrologic connectivity between land and rivers (Figure 6) (Chen et al., 2023; Mzobe et al., 2020). Riverine DOC serves as a vital source of carbon for biogeochemical processes involved in

greenhouse gas production. Hydrologic and climatic controls, including water temperature and runoff, were identified as the major factors in controlling riverine pCH_4 and pCO_2 (Figures 3 and 6). We found that increased precipitation during the wet season led to higher discharge and runoff, which mobilized previously accumulated DOC and/or soil CO_2 and CH_4 from wetlands and upland soils into streams (Raymond et al., 2016), resulting in greater CO_2 and CH_4 production within and input into the streams and, accordingly, significantly higher pCO_2 and pCH_4 (Figure 2). Moreover, the higher discharge during the wet season suggests increased near-surface turbulence and therefore higher k values, which also contributed to the higher emission rates. Temperature is another important driver for the seasonal differences in CO_2 and CH_4 dynamics. Higher temperatures could enhance the respiration rate of organic matter (Ludwig et al., 2022) and the rates of methanogenesis (Yvon-Durocher et al., 2014), creating favorable conditions for CO_2 and CH_4 production during the wet season.

Apart from geomorphologic drivers, catchments dominated by urban and agricultural land uses are typically characterized by high nutrient loadings (Park et al., 2018; Xu et al., 2024), which in turn affect surface water pCO_2 and pCH_4. This land use effect is clearly observed in the small streams within the PRB (Figures 2b–2d and, 2f, and 2h). Together, geomorphologic, hydroclimatic, and land use conditions can also alter soil characteristics, such as soil erosion rate and R_h (García-Ruiz et al., 2015; Hursh et al., 2017). R_h affects the decomposition of soil organic carbon (SOC), which represents a significant portion of soil respiration and serves as a notable source of soil CO_2 (Schindlbacher et al., 2009). Soil respiration has been widely recognized as a major contributor to stream water CO_2 (Horgby et al., 2019). In this study, R_h exhibited a close relationship with SOC, whereas SOC was negatively correlated with catchment elevation (Figure S4 in Supporting Information S1), highlighting the influence of geomorphologic factors on soil characteristics (Figure 6). This, in turn, affects the amount of SOC input into rivers and the concentration of riverine DOC (Chen et al., 2023). The positive effect of DOC on pCO_2 (Figure 3a) can be attributed to its role as a substrate for in-stream respiration, as well as the concurrent delivery of DOC and CO_2 from riparian soils or wetlands (Borges, Darchambeau, et al., 2015; Hutchins et al., 2019).

Aquatic primary productivity plays an essential role in carbon biogeochemical cycling (Battin et al., 2023; Butman et al., 2016). Chl *a*, a proxy for aquatic productivity and metabolism, has been reported to be positively correlated with CH_4 emissions in global lentic systems (DelSontro et al., 2018). For lotic systems, however, this positive correlation is primarily observed in urban rivers characterized by oxygen-poor and nutrient-rich environments (e.g., Tang et al., 2021). Similarly, we found a positive effect of Chl *a* on CH_4 (Figure 3b), possibly attributable to the enhanced decomposition of algal-derived organic matter (Borges et al., 2018). Chl *a* was also identified as a good predictor of dissolved CO_2 concentrations (Figure 3a), and its abundance is closely associated with aquatic productivity (Yoon et al., 2017). In addition, stable carbon isotopes can serve as indicators of aquatic primary productivity (Zhong et al., 2021). The negative correlation between pCO_2 and $\delta^{13}C_{DIC}$ (Figure S2a in Supporting Information S1), as well as DO (Figure S2b in Supporting Information S1), further demonstrates that riverine CO_2 dynamics are strongly regulated by in-stream photosynthesis and CO_2 outgassing. This is because both processes produce heavier $\delta^{13}C_{DIC}$, with photosynthesis preferably incorporating the lighter $^{12}CO_2$ and CO_2 outgassing preferably releasing the lighter $^{12}CO_2$ (Schulte et al., 2011). It is worth noting that catchment lithology might have complicated the $\delta^{13}C_{DIC}$ values, as supported by the significantly negative correlation between $\delta^{13}C_{DIC}$ and SiO_3^{2-} ($R^2 = 0.05$, $p < 0.01$; Figure S4 in Supporting Information S1), which is typically a major byproduct of silicate weathering. This correlation suggests that lithology may presumably play a critical role in shaping DIC dynamics and, consequently, exerts an influence on riverine pCO_2. Furthermore, in contrast to the recently reported distal processes (i.e., upstream and terrestrial production) in controlling riverine CO_2 dynamics (Gutierrez-Canovas et al., 2024), our findings indicate a combined influence of both local (i.e., in situ metabolism) and distal processes that collectively govern riverine pCO_2 and pCH_4.

Several studies have found positive correlations between pCO_2 and pCH_4 in rivers (Campeau & Del Giorgio, 2014; Teodoru et al., 2014; Wallin et al., 2014). This positive relationship may be partly due to the temperature control on stream water CO_2 and CH_4 concentrations (Wallin et al., 2014), or in situ metabolism controlled by the availability of DO (Campeau & Del Giorgio, 2014), or a combination of multiple factors (e.g., wetlands, reservoirs, and hydrology) that determine the gaseous dynamics (Teodoru et al., 2014). In our study, we found a statistically significant but weak positive correlation between pCO_2 and pCH_4 for all rivers ($R^2 = 0.10$, $p < 0.001$; Figure S2c in Supporting Information S1), which indicates that dissolved CO_2 and CH_4 shared similar combined effects of environmental factors as discussed above. Previous studies have also observed a less common negative correlation between dissolved CO_2 and CH_4 concentrations in rivers (Bai et al., 2022; Borges, Abril, et al., 2015). This negative correlation was attributed to strong CO_2 production from CH_4 oxidation and/or

aerobic respiration of organic matter (Borges, Abril, et al., 2015; Sawakuchi et al., 2016), and the redissolution of CH_4 bubbles as they migrate upwards in the water column (Maeck et al., 2014).

4.2. Role of Anthropogenic Activities and Hydrology in Modulating CO_2 and CH_4 Dynamics

Rivers and streams with a higher proportion of urban and agricultural land uses have recently been recognized as significant hotspots for CO_2 and CH_4 emissions (Brown et al., 2023; Xu et al., 2024). Agricultural and urban streams are typically characterized by elevated nutrient levels (e.g., NO_3^-, TN, and TP) and organic matter compared to forested streams (Brown et al., 2023; Zhang et al., 2021). We observed an increase in NO_3^- with increasing proportions of urban and agricultural land uses ($R^2 = 0.18$, $p < 0.001$), which indicates an increasing nutrient supply from human land uses. The effect of NO_3^- on pCO_2 is generally positive (e.g., Wang et al., 2023), consistent with the positive correlation we found between NO_3^- and pCO_2 in the dry season ($p < 0.001$, figure not presented). However, unlike CO_2, the correlation between NO_3^- and CH_4 concentrations can be either positive or negative due to the complex effects of NO_3^- on microbial processes (Stanley et al., 2016). In our study, there was no discernible relationship between NO_3^- and pCH_4 in both seasons, aligning with previous findings that highlight the intricate effects of NO_3^- on CH_4 dynamics.

Furthermore, previous studies have observed that increased water pollution, particularly from inadequately treated wastewater in urban areas, can contribute to amplified monsoonal peaks in pCO_2 and pCH_4 (Begum et al., 2021; Park et al., 2018). These peaks have been related to the direct release of dissolved CO_2, labile OM, and nutrients into urban rivers and to the anaerobic conditions typical of wastewater (Park et al., 2018). We found significant positive correlations between TN and both pCO_2 and pCH_4, and between TP and pCO_2 (Figure S4 in Supporting Information S1). Nevertheless, TN and TP were not identified as primary predictors for riverine pCO_2 and pCH_4 as previously expected (Stanley et al., 2023; Upadhyay et al., 2023). Their effects may have been masked by the influence of in-stream metabolism, as evidenced by the significant negative relationships between DO and both TN and TP (Figure S4 in Supporting Information S1).

In addition to nutrient availability, the supply of DOC has emerged as another significant factor contributing to high GHG fluxes in catchments with a higher proportion of urban and agricultural land uses (Tang et al., 2021). When compared to larger rivers, small streams generally exhibit stronger hydrologic connections to surrounding riparian zones and groundwater (Marx et al., 2017). This is consistent with the observed significantly higher pCO_2 levels in urban streams (NSH and LJ) and agricultural streams (XJH) compared with forested streams (XJX) during the wet season (Figure 2b). However, during the dry season and except for LJ, there were no significant differences in pCO_2 between urban and agricultural streams (NSH and XJH) and forested streams (XJX) (Figure 2d). One possible reason for this discrepancy is the higher availability of DOC in the wet season, facilitated by enhanced connectivity and increased runoff conditions, which may have led to the flushing of anthropogenically derived DOC into the streams (Fasching et al., 2016; Zhou et al., 2021) (Figure S5 in Supporting Information S1). These results demonstrate the combined effect of flow regime and land use on surface water pCO_2.

We also observed an increasing trend in pCO_2 and pCH_4 from upstream to downstream in the NSH rivers (Figures S6a and b in Supporting Information S1). Although similar trends have also been found in other urban rivers (e.g., Li et al., 2020) due largely to wastewater inputs or in-stream metabolism, these trends are likely to be local phenomena influenced by in-stream metabolism processes, as supported by the opposite trend of DO (Figure S6c in Supporting Information S1) and similar trend of DOC (Figure S6d in Supporting Information S1; Park et al., 2023), as well as geomorphological conditions (i.e., higher pCH_4 for NSH7 than NSH6 in the dry season due to variability in flow velocity). In addition to land use changes, construction of dams in recent decades has emerged as another significant human disturbance to riverine carbon emissions (Maavara et al., 2020; Wang et al., 2024). Apart from the well-known variations in carbon biogeochemical processes (e.g., photosynthesis and respiration) caused by increased nutrient residence times (Maavara et al., 2020), damming can also substantially alter the rates of CO_2 and CH_4 emissions by regulating gas transfer velocity through modified flow turbulence (Raymond et al., 2012). Furthermore, damming influences the seasonality of CO_2 and CH_4 fluxes by controlling near-surface turbulence and stream width, and subsequent variations in total water surface area (Calamita et al., 2021; Maavara et al., 2020). These damming effects align well with the observed decline in riverine CO_2 fluxes in northwest China, mainly attributed to the reduction in river water surface area resulting from dam

construction and excessive water withdrawals, as well as the decreased near-surface turbulence and gas transfer velocity (Ran et al., 2021).

4.3. Climate Impacts on Riverine Carbon Emissions and Future Implications

Interestingly, while both CO_2 and CH_4 production appeared to be influenced by temperature (Campeau & Del Giorgio, 2014; Ludwig et al., 2022), T_w was identified as a significant predictor only for pCH_4 (Figure 3). Additionally, we observed stronger seasonality in pCH_4 compared with pCO_2 with the median pCH_4 in the wet season nearly three times (2.9) higher than that in the dry season, which is higher than the seasonality observed for pCO_2 (2.1; Figure 2). This finding is consistent with previous studies showing that, compared to CO_2, CH_4 production is more sensitive to temperature changes due to the different kinetics of methanogenesis and organic matter respiration (Chen, Xu, et al., 2021; Yvon-Durocher et al., 2014). The relatively weak temperature sensitivity of CO_2 has also been observed in boreal rivers (Gutierrez-Canovas et al., 2024; Hutchins et al., 2019). Besides the varying activation energies that serve as indicators of the temperature-dependent response of biotic and abiotic processes related to CO_2 and CH_4 emissions (Chen, Xu, et al., 2021), the diverse sources of riverine CO_2 (e.g., groundwater input, organic matter respiration, and aquatic photosynthesis) may have also contributed to the weaker sensitivity of CO_2 production to temperature (Campeau & Del Giorgio, 2014). Our constructed model further suggests that elevated temperatures can considerably increase pCH_4, particularly at higher temperatures (Figure 5), while DO has a relatively weak effect on pCH_4. Nevertheless, this does not imply that in-stream metabolism is not a major driver for pCH_4, because Chl *a* has also been identified as a significant predictor. The greater sensitivity of CH_4 to temperature compared to CO_2 demonstrates that CH_4 is more likely to undergo substantial shifts under future climate change.

A recent study utilizing deep learning on compiled data from nearly 800 rivers across the United States and Central Europe reveals a projected deoxygenation rate of -0.038 ± 0.026 mg l^{-1} decade^{-1} and a warming rate of 0.19 ± 0.087°C decade^{-1} for rivers (Zhi et al., 2023). According to our constructed model (Figure 5), these projected changes in DO and water temperature would lead to an increase in future CH_4 production and emission. The elevated CH_4 emissions would be particularly pronounced during the summer months due to the stronger temperature sensitivity. Urban rivers, which experience the highest warming rate (Zhi et al., 2023), along with relatively oxygen-poor conditions, would become even greater hotspots for CH_4 emissions under future climate change. In contrast, our findings suggest that the projected temperature increase would have a relatively weaker impact on riverine CO_2 emissions, due to the interplay among multiple influencing factors as discussed earlier (Figures 3 and 6) (Campeau & Del Giorgio, 2014). However, the projected temperature increase is expected to be accompanied by an increase in precipitation within the PRB (RCP4.5 and RCP8.5 scenarios; Duan et al., 2021). This combined increase in temperature and the higher frequency of extreme precipitation events are likely to result in greater carbon inputs into rivers due to enhanced terrestrial production, soil erosion, and land–river connectivity (Li & Fang, 2016), potentially leading to an overall increase in riverine CO_2 production, transport, and emissions. Yet, stronger CO_2 production resulting from increased respiration rates could potentially be balanced by enhanced aquatic photosynthesis (Demars et al., 2016). Such complex and multifaceted effects of climate change on stream CO_2 dynamics warrant further investigations.

It is important to emphasize that the primary controlling factor in regulating riverine pCO_2 and pCH_4 is river ecosystem metabolism. Other factors, including geomorphology, land use, and hydrological connections, are intricately linked to nutrient and carbon (i.e., different carbon species) inputs into rivers, thereby modulating aquatic ecosystem metabolism and water chemistry. These catchment-specific factors exhibit distinct characteristics that contribute to the dynamic nature of aquatic ecosystem metabolism, resulting in significant spatial and temporal variability in riverine CO_2 and CH_4 dynamics (Battin et al., 2023). Furthermore, it is noteworthy that the observed pCO_2 and pCH_4 levels in the Pearl River system are limited to discrete daytime sampling. Recent research has underscored the diel fluctuation in CO_2 and CH_4 concentrations and emissions attributed to variations in light availability and temperature in inland waters (e.g., Chen, Wang, et al., 2021; Gómez-Gener et al., 2021; Potter & Xu, 2023). For instance, a global study revealed that the nocturnal CO_2 emissions from rivers were 27% higher than those estimated using diurnal CO_2 data only, which is primarily due to light availability (Gómez-Gener et al., 2021). Given the likely substantial diel changes in pCO_2 and pCH_4 within subtropical rivers, especially during summer months (Potter & Xu, 2023; Reiman & Xu, 2018; Zhang, Li, et al., 2020), future research in the Pearl River system is needed to mechanistically understand the diel variation in its dissolved CO_2 and CH_4 dynamics.

5. Conclusions

This study provides, for the first time, a comprehensive examination of basin-wide influencing factors for carbon emissions in the subtropical monsoon PRB. Our results demonstrate that the spatial and temporal variations in riverine CO_2 and CH_4 concentrations are governed by catchment geomorphology, soil characteristics, land use, hydrology, and climate, all of which control in-stream metabolism and biogeochemical processes. Given the intercorrelation among these factors, disentangling their individual roles in regulating riverine carbon dynamics poses a significant challenge. Our findings indicate that land use is a major predictor for both pCO_2 and pCH_4, while temperature exerts significant effects solely on CH_4. Moreover, the robustness of the model across diverse catchments suggests the wide applicability of the model in simulating the effects of land use and water temperature on pCO_2 and pCH_4. The remarkable predictive capability of the multiple linear regression models explicitly suggests that they are powerful tools for future predictions of pCO_2 and pCH_4 in the Pearl River system as well as in other subtropical monsoon rivers. With ongoing urbanization and projected future warming worldwide, our research highlights the likelihood of enhanced CH_4 and CO_2 emissions from river systems. However, the increase in CO_2 may not be as pronounced as that in CH_4. Future studies incorporating measurements with higher spatial and temporal resolution (including diel fluctuation) as well as investigations into CH_4 ebullition can offer further insights into the intricate relationships between anthropogenic perturbations, climate, and riverine carbon emissions.

Conflict of Interest

The authors declare no conflicts of interest relevant to this study.

Data Availability Statement

The dataset for riverine pCO_2 and pCH_4 in the Pearl River Basin is available at https://doi.org/10.25442/hku.24548485.

Acknowledgments
This work was supported financially by the Research Grants Council of Hong Kong (Grant 17300621 and 17306224) and the National Natural Science Foundation of China (Grant 42222062). CD is funded by an Australian Research Council grant (DE220100852).

References

Allen, G. H., & Pavelsky, T. M. (2018). Global extent of rivers and streams. *Science*, *361*(6402), 585–588. https://doi.org/10.1126/science.aat0636

Bai, X., He, Q., Li, H., Xu, Q., & Cheng, C. (2022). Response of CO_2 and CH_4 transport to damming: A case study of yulin river in the three gorges reservoir, China. *Environmental Research*, *208*, 112733. https://doi.org/10.1016/j.envres.2022.112733

Barton, K., & Barton, M. K. (2015). Package 'mumin. *Versiones*, *1*(18), 439.

Battin, T. J., Lauerwald, R., Bernhardt, E. S., Bertuzzo, E., Gener, L. G., Hall, R. O., Jr., et al. (2023). River ecosystem metabolism and carbon biogeochemistry in a changing world. *Nature*, *613*(7944), 449–459. https://doi.org/10.1038/s41586-022-05500-8

Begum, M. S., Bogard, M. J., Butman, D. E., Chea, E., Kumar, S., Lu, X., et al. (2021). Localized pollution impacts on greenhouse gas dynamics in three anthropogenically modified Asian river systems. *Journal of Geophysical Research: Biogeosciences*, *126*(5), e2020JG006124. https://doi.org/10.1029/2020jg006124

Borges, A. V., Abril, G., Darchambeau, F., Teodoru, C. R., Deborde, J., Vidal, L. O., et al. (2015). Divergent biophysical controls of aquatic CO_2 and CH_4 in the World's two largest rivers. *Scientific Reports*, *5*(1), 15614. https://doi.org/10.1038/srep15614

Borges, A. V., Darchambeau, F., Teodoru, C. R., Marwick, T. R., Tamooh, F., Geeraert, N., et al. (2015). Globally significant greenhouse-gas emissions from African inland waters. *Nature Geoscience*, *8*(8), 637–642. https://doi.org/10.1038/ngeo2486

Borges, A. V., Speeckaert, G., Champenois, W., Scranton, M. I., & Gypens, N. (2018). Productivity and temperature as drivers of seasonal and spatial variations of dissolved methane in the Southern Bight of the North Sea. *Ecosystems*, *21*(4), 583–599. https://doi.org/10.1007/s10021-017-0171-7

Brown, A. M., Bass, A. M., Skiba, U., MacDonald, J. M., & Pickard, A. E. (2023). Urban landscapes and legacy industry provide hotspots for riverine greenhouse gases: A source-to-sea study of the river clyde. *Water Research*, *236*, 119969. https://doi.org/10.1016/j.watres.2023.119969

Butman, D., & Raymond, P. A. (2011). Significant efflux of carbon dioxide from streams and rivers in the United States. *Nature Geoscience*, *4*(12), 839–842. https://doi.org/10.1038/ngeo1294

Butman, D., Stackpoole, S., Stets, E., McDonald, C. P., Clow, D. W., & Striegl, R. G. (2016). Aquatic carbon cycling in the conterminous United States and implications for terrestrial carbon accounting. *Proceedings of the National Academy of Sciences*, *113*(1), 58–63. https://doi.org/10.1073/pnas.1512651112

Calamita, E., Siviglia, A., Gettel, G. M., Franca, M. J., Winton, R. S., Teodoru, C. R., et al. (2021). Unaccounted CO_2 leaks downstream of a large tropical hydroelectric reservoir. *Proceedings of the National Academy of Sciences*, *118*(25), e2026004118. https://doi.org/10.1073/pnas.2026004118

Campeau, A., & Del Giorgio, P. A. (2014). Patterns in CH_4 and CO_2 concentrations across boreal rivers: Major drivers and implications for fluvial greenhouse emissions under climate change scenarios. *Global Change Biology*, *20*(4), 1075–1088. https://doi.org/10.1111/gcb.12479

Campeau, A., Lapierre, J.-F., Vachon, D., & del Giorgio, P. A. (2014). Regional contribution of CO_2 and CH_4 fluxes from the fluvial network in a lowland boreal landscape of Québec. *Global Biogeochemical Cycles*, *28*(1), 57–69. https://doi.org/10.1002/2013gb004685

Chen, H., Xu, X., Fang, C., Li, B., & Nie, M. (2021). Differences in the temperature dependence of wetland CO_2 and CH_4 emissions vary with water table depth. *Nature Climate Change*, *11*(9), 766–771. https://doi.org/10.1038/s41558-021-01108-4

Chen, S., Ran, L., Zhong, J., Liu, B., Yang, X., Yang, P., et al. (2024). Magnitude of and hydroclimatic controls on CO_2 and CH_4 emissions in the subtropical monsoon Pearl River Basin. *Journal of Geophysical Research: Biogeosciences*, *129*(5), e2023JG007967. https://doi.org/10.1029/2023jg007967

Chen, S., Wang, D., Ding, Y., Yu, Z., Liu, L., Li, Y., et al. (2021). Ebullition controls on CH_4 emissions in an urban, eutrophic river: A potential time-scale bias in determining the aquatic CH_4 flux. *Environmental Science and Technology*, *55*(11), 7287–7298. https://doi.org/10.1021/acs.est.1c00114

Chen, S., Zhong, J., Ran, L., Yi, Y., Wang, W., Yan, Z., et al. (2023). Geomorphologic controls and anthropogenic impacts on dissolved organic carbon from mountainous rivers: Insights from optical properties and carbon isotopes. *Biogeosciences*, *20*(24), 4949–4967. https://doi.org/10.5194/bg-20-4949-2023

DelSontro, T., Beaulieu, J. J., & Downing, J. A. (2018). Greenhouse gas emissions from lakes and impoundments: Upscaling in the face of global change. *Limnology and Oceanography Letters*, *3*(3), 64–75. https://doi.org/10.1002/lol2.10073

Demars, B. O. L., Gíslason, G. M., Ólafsson, J. S., Manson, J. R., Friberg, N., Hood, J. M., et al. (2016). Impact of warming on CO_2 emissions from streams countered by aquatic photosynthesis. *Nature Geoscience*, *9*(10), 758–761. https://doi.org/10.1038/ngeo2807

Du, Y., Chen, F., Zhang, Y., He, H., Wen, S., Huang, X., et al. (2023). Human activity coupled with climate change strengthens the role of lakes as an active pipe of dissolved organic matter. *Earth's Future*, *11*(9), e2022EF003412. https://doi.org/10.1029/2022ef003412

Duan, R., Huang, G., Zhou, X., Li, Y., & Tian, C. (2021). Ensemble drought exposure projection for multifactorial interactive effects of climate change and population dynamics: Application to the Pearl River Basin. *Earth's Future*, *9*(8). https://doi.org/10.1029/2021ef002215

Duvert, C., Butman, D. E., Marx, A., Ribolzi, O., & Hutley, L. B. (2018). CO_2 evasion along streams driven by groundwater inputs and geomorphic controls. *Nature Geoscience*, *11*(11), 813–818. https://doi.org/10.1038/s41561-018-0245-y

Eccles, R., Zhang, H., & Hamilton, D. (2019). A review of the effects of climate change on riverine flooding in subtropical and tropical regions. *Journal of Water and Climate Change*, *10*(4), 687–707. https://doi.org/10.2166/wcc.2019.175

Fasching, C., Ulseth, A. J., Schelker, J., Steniczka, G., & Battin, T. J. (2016). Hydrology controls dissolved organic matter export and composition in an Alpine stream and its hyporheic zone. *Limnology & Oceanography*, *61*(2), 558–571. https://doi.org/10.1002/lno.10232

Freychet, N., Hegerl, G., Mitchell, D., & Collins, M. (2021). Future changes in the frequency of temperature extremes may be underestimated in tropical and subtropical regions. *Communications Earth & Environment*, *2*(1), 28. https://doi.org/10.1038/s43247-021-00094-x

García-Ruiz, J. M., Beguería, S., Nadal-Romero, E., González-Hidalgo, J. C., Lana-Renault, N., & Sanjuán, Y. (2015). A meta-analysis of soil erosion rates across the world. *Geomorphology*, *239*, 160–173. https://doi.org/10.1016/j.geomorph.2015.03.008

Gómez-Gener, L., Rocher-Ros, G., Battin, T., Cohen, M. J., Dalmagro, H. J., Dinsmore, K. J., et al. (2021). Global carbon dioxide efflux from rivers enhanced by high nocturnal emissions. *Nature Geoscience*, *14*(5), 1–6. https://doi.org/10.1038/s41561-021-00722-3

Gutierrez-Canovas, C., von Schiller, D., Pace, G., Gomez-Gener, L., & Pascoal, C. (2024). Multiple stressors alter greenhouse gas concentrations in streams through local and distal processes. *Global Change Biology*, *30*(5), e17301. https://doi.org/10.1111/gcb.17301

Herrero Ortega, S., Romero Gonzalez-Quijano, C., Casper, P., Singer, G. A., & Gessner, M. O. (2019). Methane emissions from contrasting urban freshwaters: Rates, drivers, and a whole-city footprint. *Global Change Biology*, *25*(12), 4234–4243. https://doi.org/10.1111/gcb.14799

Horgby, Å., Boix Canadell, M., Ulseth, A. J., Vennemann, T. W., & Battin, T. J. (2019). High-resolution spatial sampling identifies groundwater as driver of CO_2 dynamics in an alpine stream network. *Journal of Geophysical Research: Biogeosciences*, *124*(7), 1961–1976. https://doi.org/10.1029/2019jg005047

Hursh, A., Ballantyne, A., Cooper, L., Maneta, M., Kimball, J., & Watts, J. (2017). The sensitivity of soil respiration to soil temperature, moisture, and carbon supply at the global scale. *Global Change Biology*, *23*(5), 2090–2103. https://doi.org/10.1111/gcb.13489

Hutchins, R. H. S., Prairie, Y. T., & del Giorgio, P. A. (2019). Large-scale landscape drivers of CO_2, CH_4, DOC, and DIC in boreal river networks. *Global Biogeochemical Cycles*, *33*(2), 125–142. https://doi.org/10.1029/2018gb006106

Johnson, M. S., Matthews, E., Bastviken, D., Deemer, B., Du, J., & Genovese, V. (2021). Spatiotemporal methane emission from global reservoirs. *Journal of Geophysical Research: Biogeosciences*, *126*(8). https://doi.org/10.1029/2021jg006305

Johnson, M. S., Matthews, E., Du, J., Genovese, V., & Bastviken, D. (2022). Methane emission from global lakes: New spatiotemporal data and observation-driven modeling of methane dynamics indicates lower emissions. *Journal of Geophysical Research: Biogeosciences*, *127*(7). https://doi.org/10.1029/2022jg006793

Koschorreck, M., Prairie, Y. T., Kim, J., & Marcé, R. (2021). Technical note: CO_2 is not like CH_4 – limits of and corrections to the headspace method to analyse pCO_2 in fresh water. *Biogeosciences*, *18*(5), 1619–1627. https://doi.org/10.5194/bg-18-1619-2021

Laudon, H., Buttle, J., Carey, S. K., McDonnell, J., McGuire, K., Seibert, J., et al. (2012). Cross-regional prediction of long-term trajectory of stream water DOC response to climate change. *Geophysical Research Letters*, *39*(18). https://doi.org/10.1029/2012gl053033

Lauerwald, R., Allen, G. H., Deemer, B. R., Liu, S., Maavara, T., Raymond, P., et al. (2023). Inland water greenhouse gas budgets for RECCAP2: 2. Regionalization and homogenization of estimates. *Global Biogeochemical Cycles*, *37*(5). https://doi.org/10.1029/2022gb007658

Lee, H., Calvin, K., Dasgupta, D., Krinner, G., Mukherji, A., Thorne, P., et al. (2023). Climate change 2023: Synthesis report. Contribution of working groups I, II and III to the sixth assessment report of the intergovernmental panel on climate change.

Li, X., Yao, H., Yu, Y., Cao, Y., & Tang, C. (2020). Greenhouse gases in an urban river: Trend, isotopic evidence for underlying processes, and the impact of in-river structures. *Journal of Hydrology*, *591*, 125290. https://doi.org/10.1016/j.jhydrol.2020.125290

Li, Z., & Fang, H. (2016). Impacts of climate change on water erosion: A review. *Earth-Science Reviews*, *163*, 94–117. https://doi.org/10.1016/j.earscirev.2016.10.004

Liu, S., Kuhn, C., Amatulli, G., Aho, K., Butman, D. E., Allen, G. H., et al. (2022). The importance of hydrology in routing terrestrial carbon to the atmosphere via global streams and rivers. *Proceedings of the National Academy of Sciences*, *119*(11), e2106322119. https://doi.org/10.1073/pnas.2106322119

Ludwig, S. M., Natali, S. M., Mann, P. J., Schade, J. D., Holmes, R. M., Powell, M., et al. (2022). Using machine learning to predict inland aquatic CO_2 and CH_4 concentrations and the effects of wildfires in the Yukon-Kuskokwim Delta, Alaska. *Global Biogeochemical Cycles*, *36*(4), e2021GB007146. https://doi.org/10.1029/2021gb007146

Maavara, T., Chen, Q., Van Meter, K., Brown, L. E., Zhang, J., Ni, J., & Zarfl, C. (2020). River dam impacts on biogeochemical cycling. *Nature Reviews Earth and Environment*, *1*(2), 103–116. https://doi.org/10.1038/s43017-019-0019-0

Maeck, A., Hofmann, H., & Lorke, A. (2014). Pumping methane out of aquatic sediments – Ebullition forcing mechanisms in an impounded river. *Biogeosciences*, *11*(11), 2925–2938. https://doi.org/10.5194/bg-11-2925-2014

Marx, A., Dusek, J., Jankovec, J., Sanda, M., Vogel, T., van Geldern, R., et al. (2017). A review of CO_2 and associated carbon dynamics in headwater streams: A global perspective. *Reviews of Geophysics*, *55*(2), 560–585. https://doi.org/10.1002/2016RG000547

Mwanake, R. M., Gettel, G. M., Ishimwe, C., Wangari, E. G., Butterbach-Bahl, K., & Kiese, R. (2022). Basin-scale estimates of greenhouse gas emissions from the Mara River, Kenya: Importance of discharge, stream size, and land use/land cover. *Limnology & Oceanography*, *67*(8), 1776–1793. https://doi.org/10.1002/lno.12166

Mzobe, P., Yan, Y., Berggren, M., Pilesjö, P., Olefeldt, D., Lundin, E., et al. (2020). Morphometric control on dissolved organic carbon in subarctic streams. *Journal of Geophysical Research: Biogeosciences*, *125*(9), e2019JG005348. https://doi.org/10.1029/2019jg005348

Park, J.-H., Lee, H., Zhumabieke, M., Kim, S.-H., Shin, K.-H., & Khim, B.-K. (2023). Basin-specific pollution and impoundment effects on greenhouse gas distributions in three rivers and estuaries. *Water Research*, *236*, 119982. https://doi.org/10.1016/j.watres.2023.119982

Park, J.-H., Nayna, O. K., Begum, M. S., Chea, E., Hartmann, J., Keil, R. G., et al. (2018). Reviews and syntheses: Anthropogenic perturbations to carbon fluxes in Asian river systems – Concepts, emerging trends, and research challenges. *Biogeosciences*, *15*(9), 3049–3069. https://doi.org/10.5194/bg-15-3049-2018

Potter, L., & Xu, Y. J. (2023). Can a eutrophic lake function as a carbon sink? Case study of a subtropical eutrophic lake in southern USA. *Journal of Hydrology*, *625*, 130071. https://doi.org/10.1016/j.jhydrol.2023.130071

Ran, L., Butman, D. E., Battin, T. J., Yang, X., Tian, M., Duvert, C., et al. (2021). Substantial decrease in CO_2 emissions from Chinese inland waters due to global change. *Nature Communications*, *12*(1), 1730. https://doi.org/10.1038/s41467-021-21926-6

Raymond, P. A., Hartmann, J., Lauerwald, R., Sobek, S., McDonald, C., Hoover, M., et al. (2013). Global carbon dioxide emissions from inland waters. *Nature*, *503*(7476), 355–359. https://doi.org/10.1038/nature12760

Raymond, P. A., Saiers, J. E., & Sobczak, W. V. (2016). Hydrological and biogeochemical controls on watershed dissolved organic matter transport: Pulse-shunt concept. *Ecology*, *97*(1), 5–16. https://doi.org/10.1890/14-1684.1

Raymond, P. A., Zappa, C. J., Butman, D., Bott, T. L., Potter, J., Mulholland, P., et al. (2012). Scaling the gas transfer velocity and hydraulic geometry in streams and small rivers. *Limnology and Oceanography: Fluids and Environments*, *2*(1), 41–53. https://doi.org/10.1215/21573689-1597669

R Development Core Team. (2020). *R: A language and environment for statistical computing*. R Foundation for Statistical Computing.

Regnier, P., Resplandy, L., Najjar, R. G., & Ciais, P. (2022). The land-to-ocean loops of the global carbon cycle. *Nature*, *603*(7901), 401–410. https://doi.org/10.1038/s41586-021-04339-9

Reiman, J., & Xu, Y. (2018). Diel variability of pCO_2 and CO_2 outgassing from the Lower Mississippi River: Implications for riverine CO_2 outgassing estimation. *Water*, *11*(1), 43. https://doi.org/10.3390/w11010043

Rocher-Ros, G., Stanley, E. H., Loken, L. C., Casson, N. J., Raymond, P. A., Liu, S., et al. (2023). Global methane emissions from rivers and streams. *Nature*, *621*(7979), 530–535. https://doi.org/10.1038/s41586-023-06344-6

Rosentreter, J. A., Borges, A. V., Deemer, B. R., Holgerson, M. A., Liu, S., Song, C., et al. (2021). Half of global methane emissions come from highly variable aquatic ecosystem sources. *Nature Geoscience*, *14*(4), 225–230. https://doi.org/10.1038/s41561-021-00715-2

Sanchez, G. (2013). PLS path modeling with R. *Berkeley: Trowchez Editions*, *383*(2013), 551.

Sawakuchi, H. O., Bastviken, D., Sawakuchi, A. O., Ward, N. D., Borges, C. D., Tsai, S. M., et al. (2016). Oxidative mitigation of aquatic methane emissions in large Amazonian rivers. *Global Change Biology*, *22*(3), 1075–1085. https://doi.org/10.1111/gcb.13169

Schindlbacher, A., Zechmeister-Boltenstern, S., & Jandl, R. (2009). Carbon losses due to soil warming: Do autotrophic and heterotrophic soil respiration respond equally? *Global Change Biology*, *15*(4), 901–913. https://doi.org/10.1111/j.1365-2486.2008.01757.x

Schulte, P., van Geldern, R., Freitag, H., Karim, A., Négrel, P., Petelet-Giraud, E., et al. (2011). Applications of stable water and carbon isotopes in watershed research: Weathering, carbon cycling, and water balances. *Earth-Science Reviews*, *109*(1–2), 20–31. https://doi.org/10.1016/j.earscirev.2011.07.003

Stanley, E. H., Casson, N. J., Christel, S. T., Crawford, J. T., Loken, L. C., & Oliver, S. K. (2016). The ecology of methane in streams and rivers: Patterns, controls, and global significance. *Ecological Monographs*, *86*(2), 146–171. https://doi.org/10.1890/15-1027

Stanley, E. H., Loken, L. C., Casson, N. J., Oliver, S. K., Sponseller, R. A., Wallin, M. B., et al. (2023). GRiMeDB: The global river methane database of concentrations and fluxes. *Earth System Science Data*, *15*(7), 2879–2926. https://doi.org/10.5194/essd-15-2879-2023

Tang, W., Xu, Y. J., Ma, Y., Maher, D. T., & Li, S. (2021). Hot spot of CH_4 production and diffusive flux in rivers with high urbanization. *Water Research*, *204*, 117624. https://doi.org/10.1016/j.watres.2021.117624

Teodoru, C. R., Nyoni, F. C., Borges, A. V., Darchambeau, F., Nyambe, I., & Bouillon, S. (2014). Dynamics of greenhouse gases (CO_2, CH_4, N_2O) along the Zambezi River and major tributaries, and their importance in the riverine carbon budget. *Biogeosciences*, *11*(11), 16391–16445. https://doi.org/10.5194/bgd-11-16391-2014

Tian, Q., & Yang, S. (2017). Regional climatic response to global warming: Trends in temperature and precipitation in the Yellow, Yangtze and Pearl River basins since the 1950s. *Quaternary International*, *440*, 1–11. https://doi.org/10.1016/j.quaint.2016.02.066

Upadhyay, P., Prajapati, S. K., & Kumar, A. (2023). Impacts of riverine pollution on greenhouse gas emissions: A comprehensive review. *Ecological Indicators*, *154*, 110649. https://doi.org/10.1016/j.ecolind.2023.110649

Wallin, M. B., Löfgren, S., Erlandsson, M., & Bishop, K. (2014). Representative regional sampling of carbon dioxide and methane concentrations in hemiboreal headwater streams reveal underestimates in less systematic approaches. *Global Biogeochemical Cycles*, *28*(4), 465–479. https://doi.org/10.1002/2013gb004715

Wang, J., Wang, X., Liu, T., Chen, H., He, Y., & Yuan, X. (2023). Ecological restoration effectively mitigated pCO_2 and CO_2 evasions from severely polluted urban rivers. *Journal of Geophysical Research: Biogeosciences*, *128*(11). https://doi.org/10.1029/2023jg007531

Wang, W., Li, S.-L., Zhong, J., Yi, Y., Yue, F., Han, Z., et al. (2024). Unraveling the factors influencing CO2 emissions from hydroelectric reservoirs in karst and non-karst regions: A comparative analysis. *Water Research*, *248*, 120893. https://doi.org/10.1016/j.watres.2023.120893

Xu, W., Wang, G., Liu, S., Wang, J., McDowell, W. H., Huang, K., et al. (2024). Globally elevated greenhouse gas emissions from polluted urban rivers. *Nature Sustainability*, *7*(7), 1–11. https://doi.org/10.1038/s41893-024-01358-y

Yoon, T. K., Jin, H., Begum, M. S., Kang, N., & Park, J. H. (2017). CO_2 outgassing from an urbanized River System fueled by wastewater treatment plant effluents. *Environmental Science and Technology*, *51*(18), 10459–10467. https://doi.org/10.1021/acs.est.7b02344

Yvon-Durocher, G., Allen, A. P., Bastviken, D., Conrad, R., Gudasz, C., St-Pierre, A., et al. (2014). Methane fluxes show consistent temperature dependence across microbial to ecosystem scales. *Nature*, *507*(7493), 488–491. https://doi.org/10.1038/nature13164

Zhang, L., Xia, X., Liu, S., Zhang, S., Li, S., Wang, J., et al. (2020). Significant methane ebullition from alpine permafrost rivers on the East Qinghai–Tibet Plateau. *Nature Geoscience*, *13*(5), 349–354. https://doi.org/10.1038/s41561-020-0571-8

Zhang, T., Li, J., Pu, J., Martin, J. B., Wang, S., & Yuan, D. (2020). Rainfall possibly disturbs the diurnal pattern of CO_2 degassing in the Lijiang River, SW China. *Journal of Hydrology*, *590*, 125540. https://doi.org/10.1016/j.jhydrol.2020.125540

Zhang, W., Li, H., Xiao, Q., & Li, X. (2021). Urban rivers are hotspots of riverine greenhouse gas (N_2O, CH_4, CO_2) emissions in the mixed-landscape Chaohu Lake Basin. *Water Research*, *189*, 116624. https://doi.org/10.1016/j.watres.2020.116624

Zhi, W., Klingler, C., Liu, J., & Li, L. (2023). Widespread deoxygenation in warming rivers. *Nature Climate Change*, *13*(10), 1105–1113. https://doi.org/10.1038/s41558-023-01793-3

Zhong, J., Wallin, M. B., Wang, W., Li, S.-L., Guo, L., Dong, K., et al. (2021). Synchronous evaporation and aquatic primary production in tropical river networks. *Water Research*, *200*, 117272. https://doi.org/10.1016/j.watres.2021.117272

Zhou, Y., Yao, X., Zhou, L., Zhao, Z., Wang, X., Jang, K. S., et al. (2021). How hydrology and anthropogenic activity influence the molecular composition and export of dissolved organic matter: Observations along a large river continuum. *Limnology & Oceanography*, *66*(5), 1730–1742. https://doi.org/10.1002/lno.11716

Zhu, Y., Jones, J. I., Collins, A. L., Zhang, Y., Olde, L., Rovelli, L., et al. (2022). Separating natural from human enhanced methane emissions in headwater streams. *Nature Communications*, *13*(1), 3810. https://doi.org/10.1038/s41467-022-31559-y

Zuur, A. F., Ieno, E. N., & Elphick, C. S. (2010). A protocol for data exploration to avoid common statistical problems. *Methods in Ecology and Evolution*, *1*(1), 3–14. https://doi.org/10.1111/j.2041-210X.2009.00001.x

References From the Supporting Information

Borrelli, P., Ballabio, C., Yang, J. E., Robinson, D. A., & Panagos, P. (2022). GloSEM: High-resolution global estimates of present and future soil displacement in croplands by water erosion. *Scientific Data*, *9*(1), 406. https://doi.org/10.1038/s41597-022-01489-x

Gong, P., Liu, H., Zhang, M., Li, C., Wang, J., Huang, H., et al. (2019). Stable classification with limited sample: Transferring a 30-m resolution sample set collected in 2015 to mapping 10-m resolution global land cover in 2017. *Science Bulletin*, *64*(6), 370–373. https://doi.org/10.1016/j.scib.2019.03.002

Hartmann, J., & Moosdorf, N. (2012). The new global lithological map database GLiM: A representation of rock properties at the earth surface. *Geochemistry, Geophysics, Geosystems*, *13*(12), Q12004. https://doi.org/10.1029/2012gc004370

Hengl, T., de Jesus, J. M., MacMillan, R. A., Batjes, N. H., Heuvelink, G. B., Ribeiro, E., et al. (2014). SoilGrids1km--global soil information based on automated mapping. *PLoS One*, *9*(8), e105992. https://doi.org/10.1371/journal.pone.0105992

Robbins, L., Hansen, M., Kleypas, J., & Meylan, S. (2010). *CO2calc: A user-friendly seawater carbon calculator for windows, mac OS X, and iOS (iPhone)*. US Department of the Interior, US Geological Survey.

Robinson, N., Regetz, J., & Guralnick, R. P. (2014). EarthEnv-DEM90: A nearly-global, void-free, multi-scale smoothed, 90m digital elevation model from fused aster and srtm data. *ISPRS Journal of Photogrammetry and Remote Sensing*, *87*, 57–67. https://doi.org/10.1016/j.isprsjprs.2013.11.002

Running, S., & Zhao, M. (2021). MODIS/Terra net primary production gap-filled yearly L4 global 500m SIN grid V061. *NASA EOSDIS Land Processes DAAC*.

Stell, E., Warner, D., Jian, J., Bond-Lamberty, B., & Vargas, R. (2021). *Global gridded 1-km soil and soil heterotrophic respiration derived from SRDB v5*. ORNL DAAC.

Sujud, L. H., & Jaafar, H. H. (2022). A global dynamic runoff application and dataset based on the assimilation of GPM, SMAP, and GCN250 curve number datasets. *Scientific Data*, *9*(1), 706. https://doi.org/10.1038/s41597-022-01834-0

Warszawski, L., Frieler, K., Huber, V., Piontek, F., Serdeczny, O., Zhang, X., et al. (2017). Center for international earth science information network—Ciesin—columbia university.(2016). Gridded population of the world, version 4 (gpwv4): Population density. Palisades. ny: Nasa socioeconomic data and applications center (sedac). https://doi.org/10.7927/h4np22dq, in *Atlas of environmental risks facing China under climate change*, edited, (p. 228).

Erratum

The originally published version of this article contained a typographical error. In the Acknowledgments, the grant number 17300624 should be changed to 17306224. The error has been corrected, and this may be considered the authoritative version of record.